

Supplemental Information

A versatile platform for generating engineered extracellular vesicles with defined therapeutic properties

Kevin Dooley, Russell E. McConnell, Ke Xu, Nuruddeen D. Lewis, Sonya Haupt, Madeleine R. Youniss, Shelly Martin, Chang Ling Sia, Christine McCoy, Raymond J. Moniz, Olga Burenkova, Jorge Sanchez-Salazar, Su Chul Jang, Bryan Choi, Rane A. Harrison, Damian Houde, Dalia Burzyn, Charan Leng, Katherine Kirwin, Nikki L. Ross, Jonathan D. Finn, Leonid Gaidukov, Kyriakos D. Economides, Scott Estes, James E. Thornton, John D. Kulman, Sriram Sathyanarayanan, and Douglas E. Williams

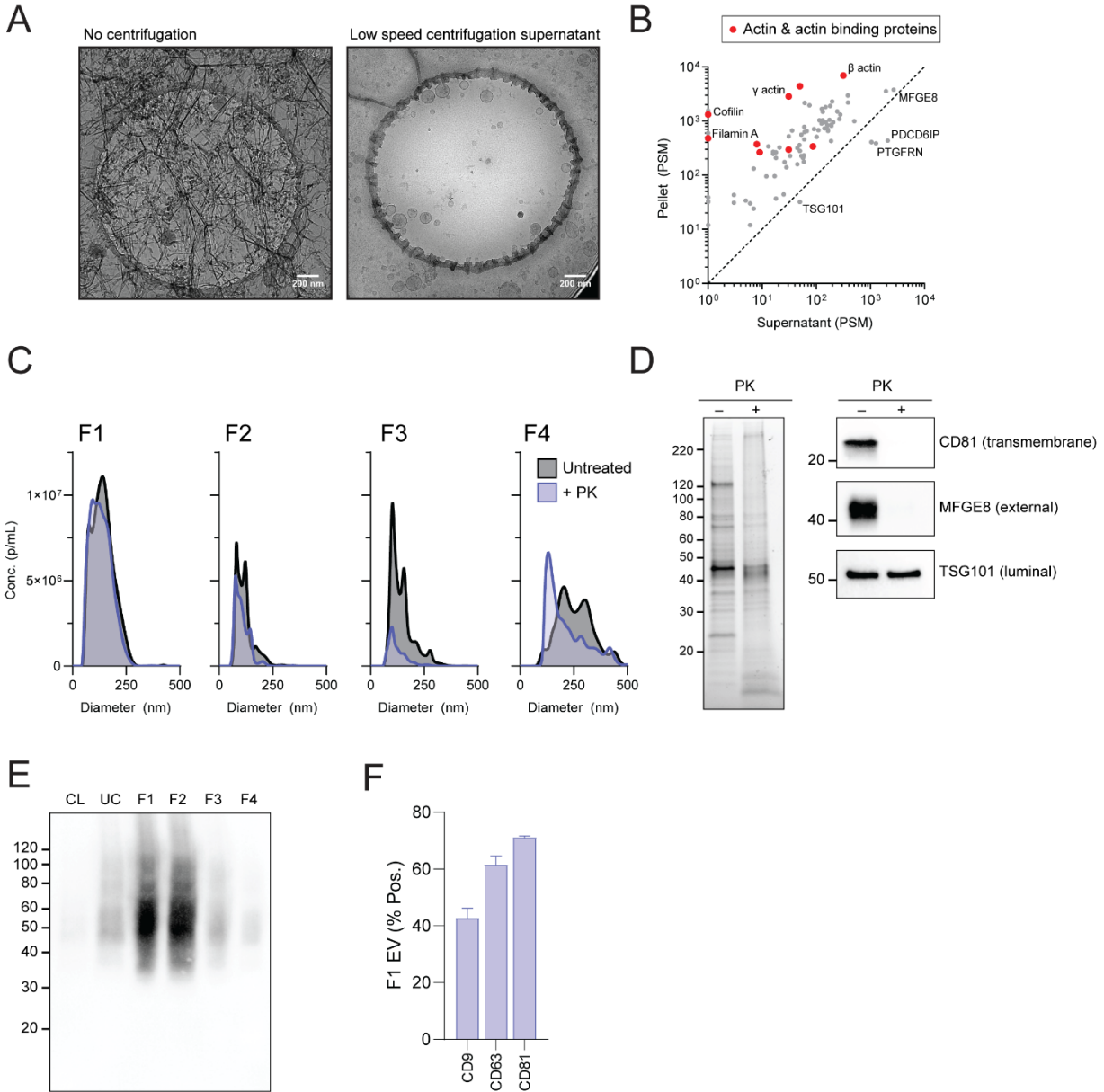


Figure S1. EV characterization. (A) Cryo-EM images of EVs purified according to the protocol in Fig. 1A with and without 20,000 x g centrifugation prior to the final pelleting step. (B) Proteomic analysis of low-speed centrifugation pellet (y-axis) and supernatant (x-axis). Actin and actin binding proteins are shown in red. PSM, peptide spectrum matches. (C) F1-F4 NTA size distributions and concentration measurements analyzed with (blue) and without (grey) proteinase K treatment. (D) SDS-PAGE and immunoblotting analysis of F1 EVs with and without proteinase K treatment. Transmembrane and external protein cargo are digested while internal cargo is protected. (E) Anti-CD63 immunoblot of F1-F4 along with the producer cell lysate (CL) and crude ultracentrifuged pellet (UC). (F) EV flow cytometry analysis for CD9, CD63, and CD81. EVs from F1 were stained with PE-conjugated antibodies targeting each tetraspanin. Unbound antibody was removed by ultracentrifugation and stained EVs were washed once with PBS prior to analysis. The percent positive for each marker are given compared to unstained EVs as mean \pm SD.

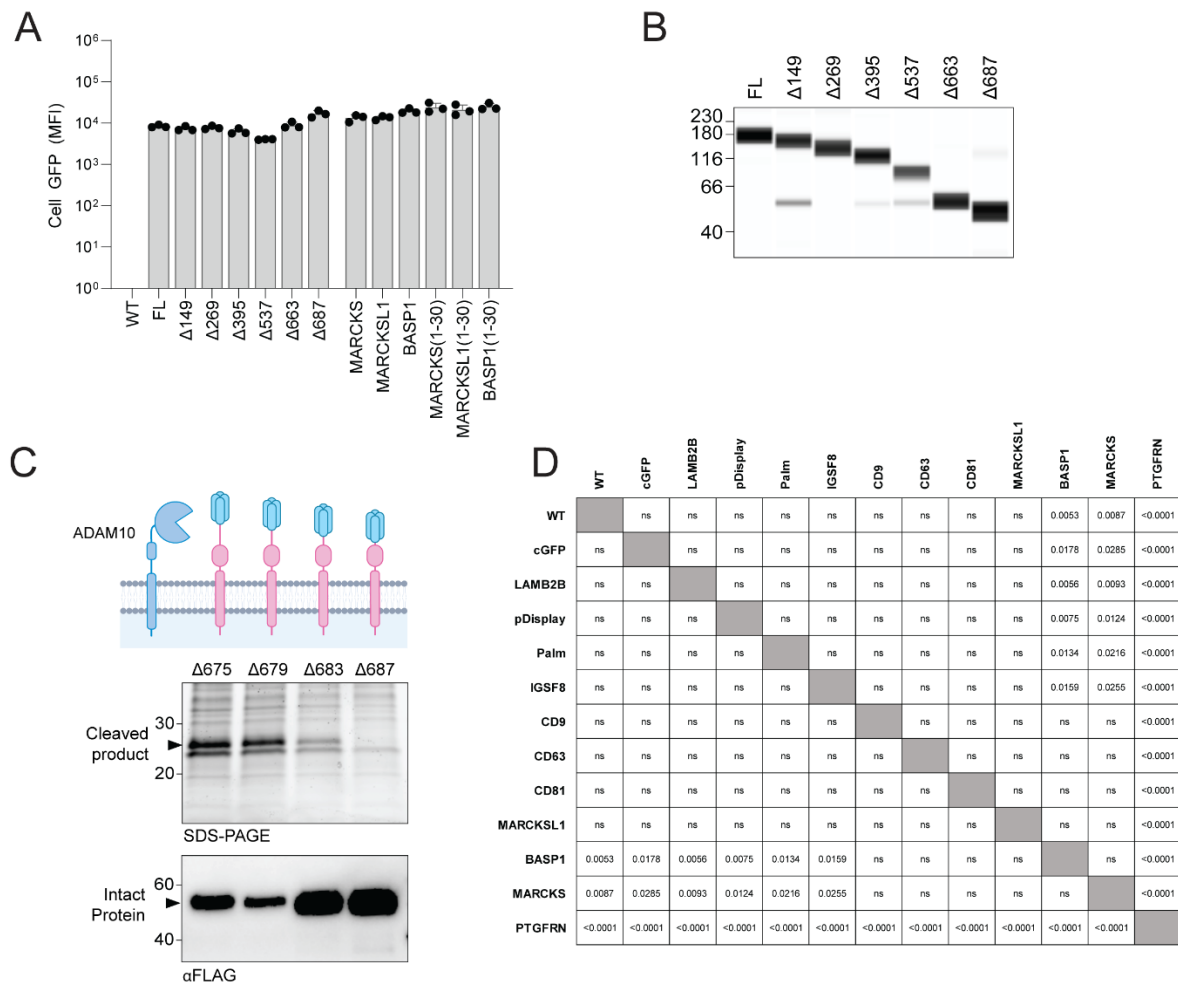


Figure S2. Characterization of scaffolds for EV engineering. (A) Cellular MFI of EV producer cells stably expressing GFP fusions to the indicated scaffold. Data from three biological replicates are plotted as mean \pm SD. (B) Anti-GFP immunoblot analysis of cell lysates from stable lines expressing truncations of PTGFRN fused to GFP. (C) Schematic of the EV membrane showing ADAM10 along with incrementally truncated forms of PTGFRN with an N-terminal fusion to FLAG-tagged IL7. SDS-PAGE analysis of purified EVs from each indicated truncation displaying FLAG-tagged IL7. The membrane bound cleaved product runs at 25 kDa as there is no C-terminal GFP fusion in these constructs. As the scaffold is shortened, the intensity of the cleaved product is diminished, with $\Delta 687$ showing no cleaved product. Anti-FLAG immunoblot on the same samples shows more intact fusion protein on the short scaffolds. (D) Statistical comparisons for data presented in Figure 2C. All comparisons were made by one-way ANOVA and Tukey's multiple comparison test. P values are shown in the table. ns, not significant.

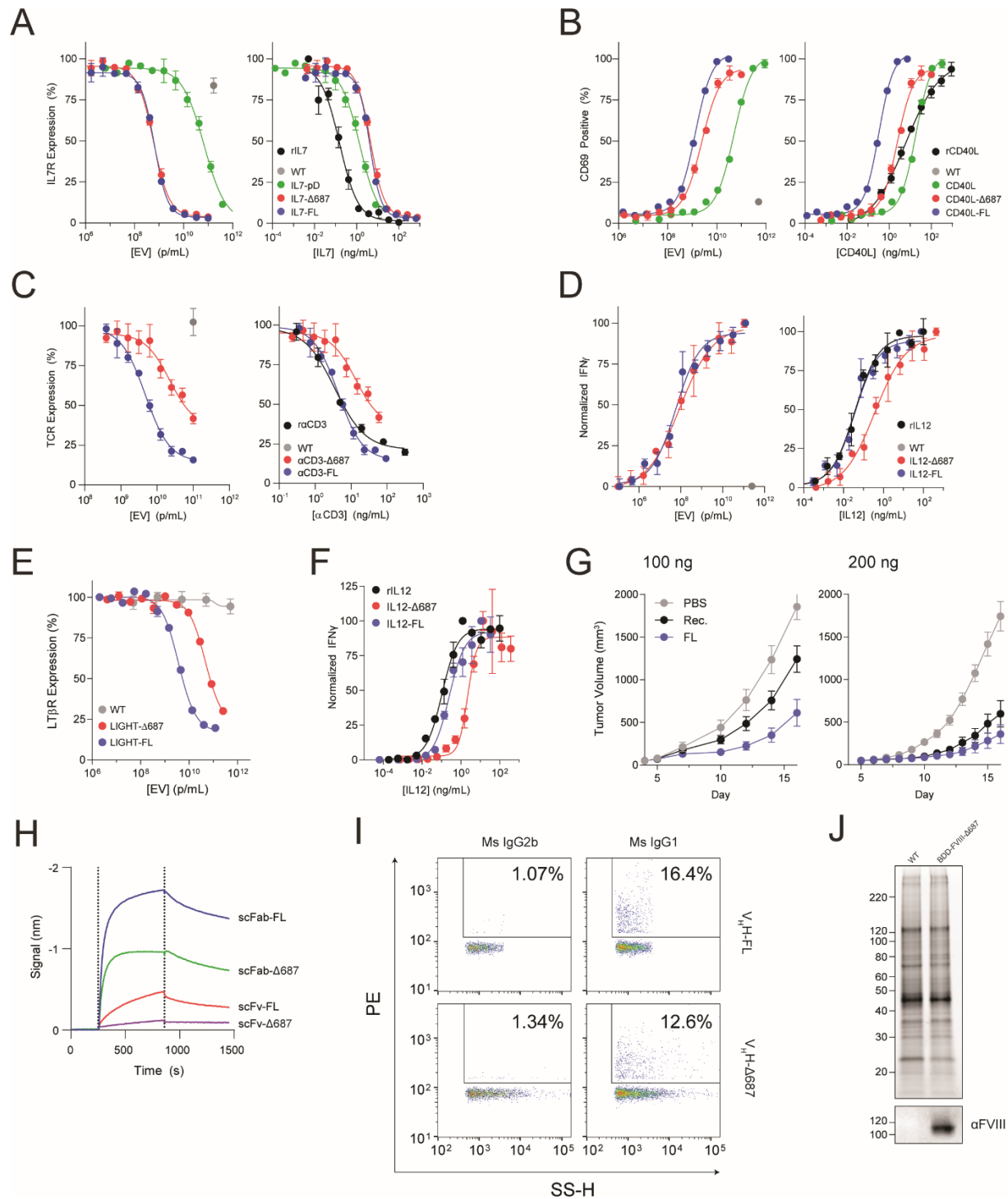


Figure S3. EV surface display. (A-D) Representative dose response curves for data presented in Fig. 4B-E, respectively (mean \pm SEM). (E) Activity of EVs displaying TNFSF ligand LIGHT on both FL and Δ 687 scaffolds was evaluated *in vitro* by measuring the downregulation of the cognate receptor, LT β R, following overnight incubation with HT-29 human colorectal adenocarcinoma epithelial cells (mean \pm SEM). (F) *In vitro* activity assessment of murine IL12 fused to FL and Δ 687 PTGFRN scaffolds (mean \pm SEM). (G) Full tumor growth curves for the data presented in Fig. 4F (mean \pm SEM). (H) Biolayer interferometry analysis of EVs displaying anti-CLEC9A scFab or scFv antibody fragments. CLEC9A-Fc fusion protein was immobilized on protein A biosensors prior to EV incubation. (I) EVs were engineered to display a single domain V $_H$ H antibody that binds to the Fc region of mouse IgG1 antibodies¹. V $_H$ H-displaying EVs were incubated with mouse IgG2b or IgG1 antibodies labeled with PE, washed, and analyzed by single particle flow cytometry. Single domain antibody fusions showed specificity for IgG1 subtype only. (J) SDS-PAGE and immunoblot analysis of EVs displaying the B domain-deleted form of FVIII (BDD-FVIII) fused to the Δ 687 scaffold.

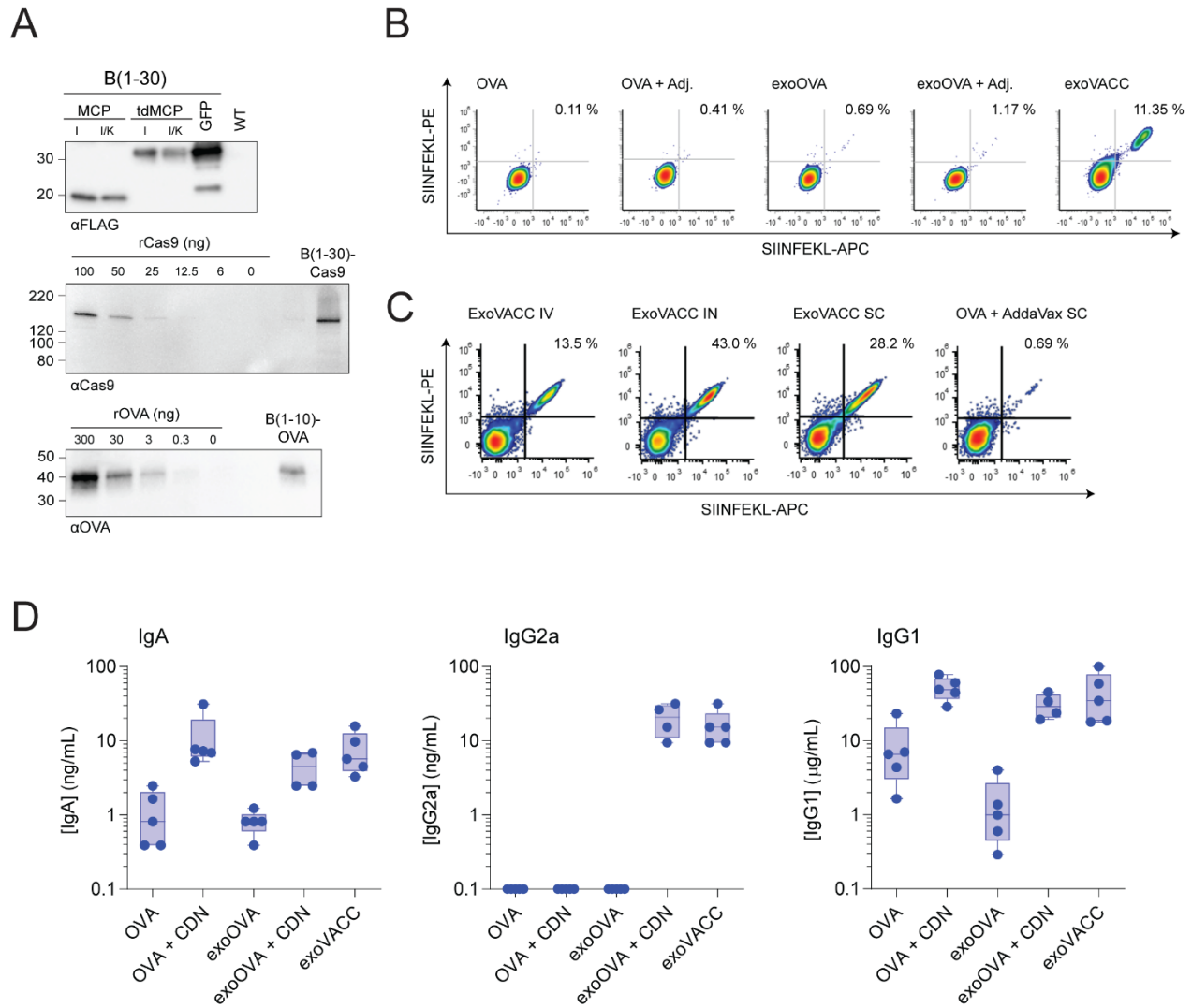


Figure S4. EV luminal loading. (A) Immunoblots on $1E+10$ purified EVs expressing truncated BASP1 fusions to RNA-binding major coat protein (MCP, top), *Streptococcus pyogenes* Cas9 (middle), and chicken ovalbumin (OVA). MCP variants with higher binding affinity for the MS2-hairpin structure were V29I (I) or V29I/N55K (I/K) expressed as monomers (MCP) or tandem dimers (tdMCP). An average of 9 molecules of Cas9 were loaded per EV. An average of 168 molecules of OVA were loaded per EV. (B-C) Representative flow plots used to generate the data in Fig. 5B and 5D, respectively, gated on effector memory T cells. (D) IgA and IgG responses from the experiment in Fig. 5C.

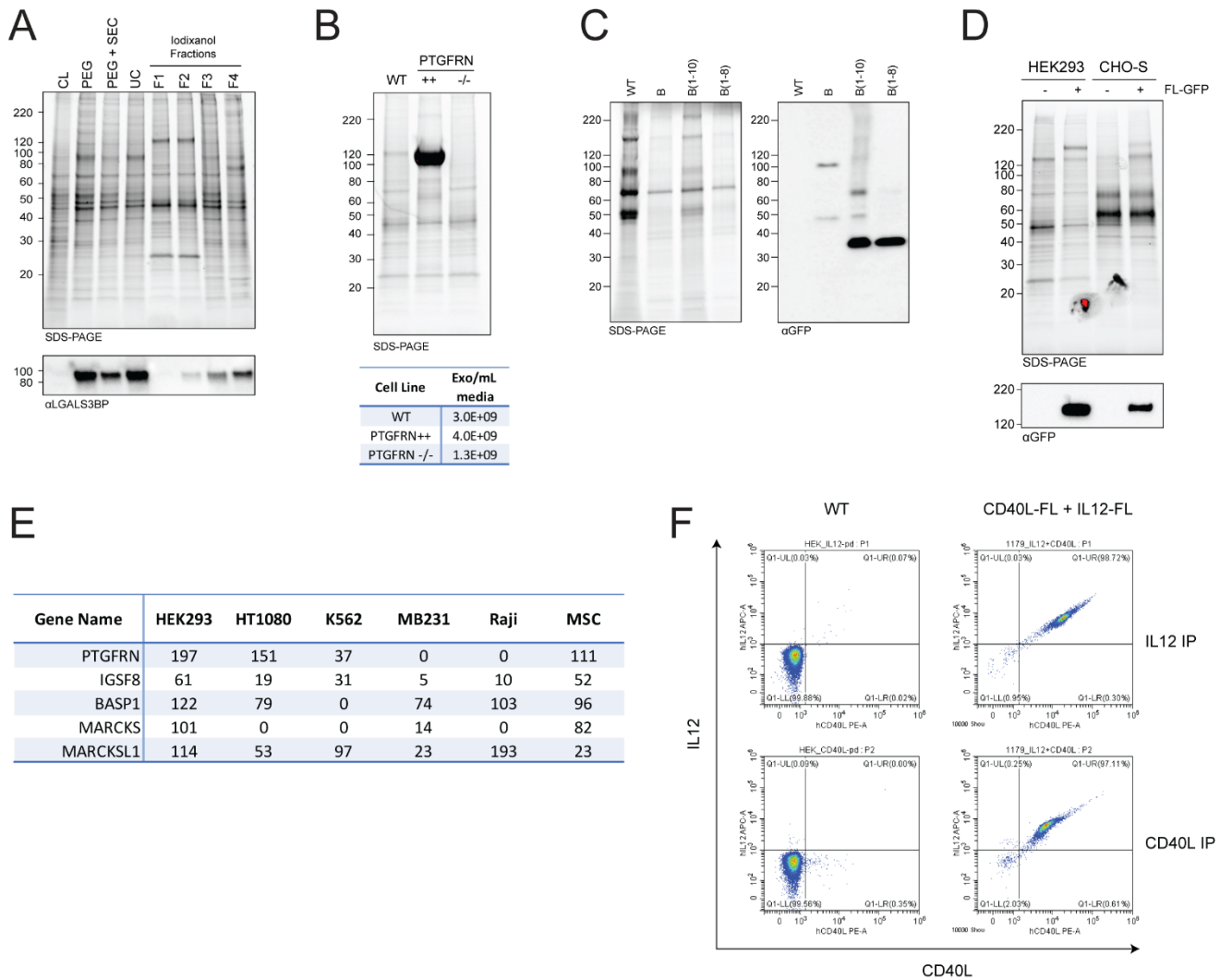


Figure S5. EV engineering platform versatility. (A) SDS-PAGE analysis of cell lysate (CL) and EVs purified by polyethylene glycol (PEG) precipitation², PEG with size exclusion chromatography (SEC), UC, and iodixanol density gradient. LGALS3BP immunoblot analysis was used as an indicator of contaminating non-vesicular material. (B) SDS-PAGE analysis of EVs overexpressing (++) or knocking out (-/-) PTGFRN alongside WT. EVs purified per volume of conditioned media is given in the table below. (C) Full length, 1-10, and 1-8 BASP1 sequences with a C-terminal GFP/FLAG fusion were transiently transfected into CHO suspension cells. 48 hours post-transfection, EVs were enriched by UC only. SDS-PAGE and anti-FLAG immunoblot analysis confirm robust transgene expression for the 1-10 and 1-8 BASP1 scaffolds. (D) Full-length PTGFRN with a C-terminal GFP/FLAG fusion was transiently transfected into HEK293 and CHO suspension cells. 48 hours post-transfection, EVs were purified using the protocol outlined in Fig. 1A. SDS-PAGE and anti-GFP immunoblot analysis show robust transgene expression in both HEK293 and CHO cell lines. (E) Quantitative peptide spectrum matches for IgSF-EWI and MARCKS family members detected in purified EV samples from the indicated cell lines purified using the protocol outlined in Fig. 1A. (F) EVs were purified from a stable cell line co-transfected with separate DNA cassettes encoding IL12 and CD40L fused to FL PTGFRN. Magnetic beads coated with either anti-IL12 (top row) or anti-CD40L (bottom row) were incubated with purified EVs overnight with mild agitation. Beads were washed, labeled with anti-IL12 APC and anti-CD40L PE antibodies and analyzed by flow cytometry.

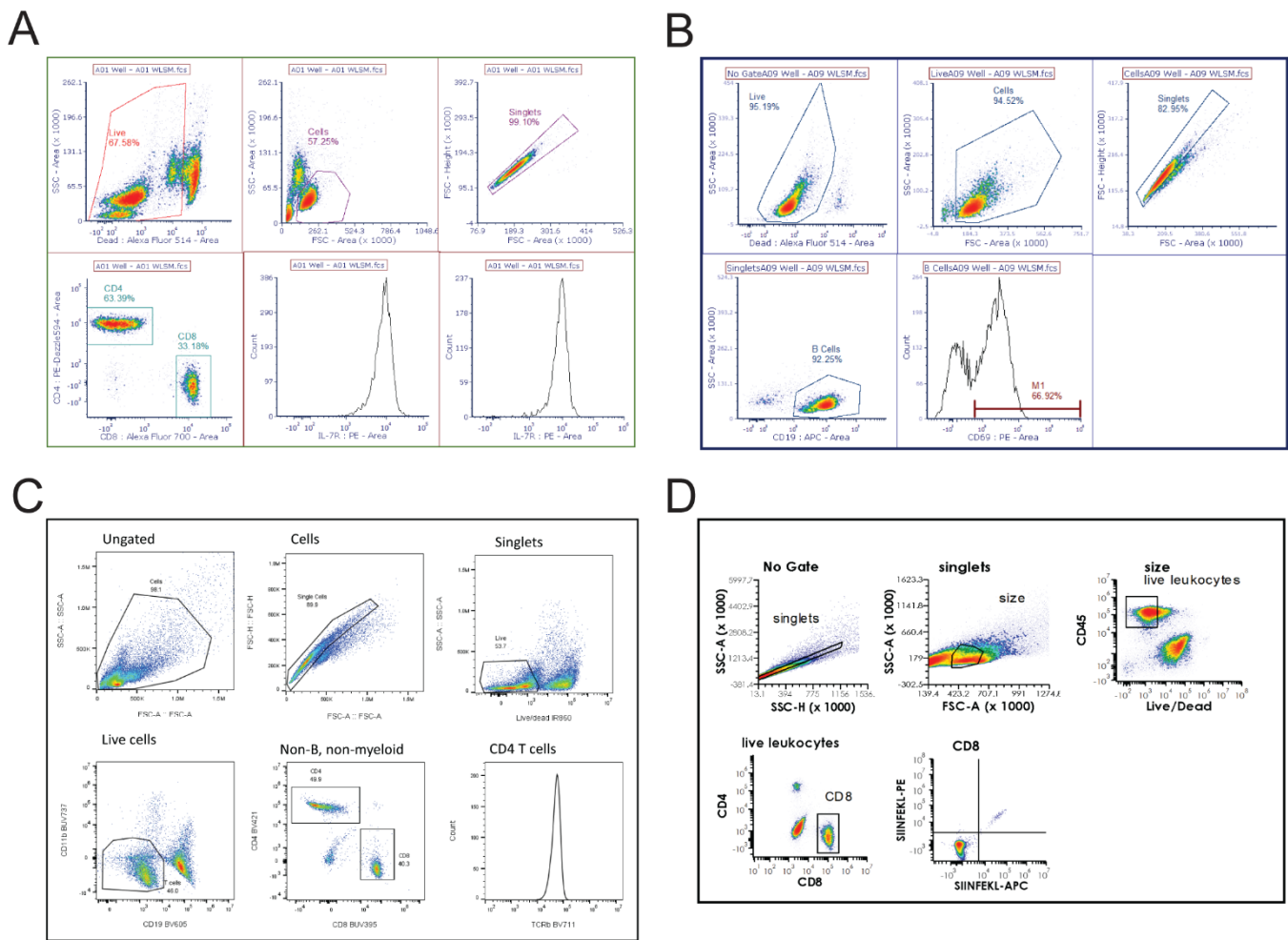


Figure S6. Gating schemes for (A) IL7, (B) CD40L, (C) α CD3, and (D) vaccination flow cytometry experiments.

Supplemental References

1. Pleiner, T., Bates, M. & Görlich, D. A toolbox of anti-mouse and anti-rabbit IgG secondary nanobodies. *J. Cell Biol.* **217**, 1143–1154 (2018).
2. Rider, M. A., Hurwitz, S. N. & Meckes, D. G. ExtraPEG: A polyethylene glycol-based method for enrichment of extracellular vesicles. *Sci. Rep.* **6**, 1–14 (2016).